



Evaluation of Polyethylene Terephthalate Microfibers as Reinforcement for High Density Polyethylene and Effect of Silane treated fibers on Properties of the Composite

M. Praharaj Bhatnagar ^{1*}, P. Mahanwar ²

^{1,2}Department of Polymer & Surface Engineering, Institute of Chemical Technology, Matunga (E),
Mumbai – 400019, India.

Received 18 June 2019,
Revised 03 Nov 2019,
Accepted 04 Nov 2019

Keywords

- ✓ PET microfiber,
- ✓ HDPE,
- ✓ Fiber composite,
- ✓ VTMO

*manojpb.ictmumbai@gmail.com

Phone: +912233612457;
Mobile: +919594382323

Abstract

In this paper, chopped PET microfiber of 6 - 7 mm length and 20 µm diameter has been used and evaluated for its reinforcing effect on high density polyethylene matrix. A microfiber composite has been prepared first by extrusion blending, where vinyl trimethoxy silane (VTMO) has been used as a coupling agent to help dispersion and improve adhesion between the PET fibers and the matrix HDPE. The composite has been injection moulded into standard specimens and tested for effect on Tensile Strength, Young's Modulus and Izod Impact Strength. Differential Scanning Calorimetry (DSC), along with Thermogravimetric Analysis (TGA) and X-ray Diffraction Spectroscopy (XRD) have been used to corroborate the morphology, obtained by Scanning Electron Microscopy (SEM). Addition of 3% VTMO treated PET fibers resulted in increasing the tensile strength by 14%.

1. Introduction

The need to have conventional polymers with enhanced mechanical properties has laid greater emphasis on plastic composite material research. Even though various natural fibers have been used for preparing composites, it has been observed that they are generally difficult to disperse and ultimately result in poor mechanical performance of the composite [1]. Lei et al. have made use of natural fibers including bagasse and wood to reinforce recycled HDPE with maleated HDPE for improving interfacial adhesion. But these natural fibers have the disadvantage of lower thermal stability and poor bio stability. They have used maleated polyethylene, carboxylated polyethylene and titanium derived coupling agent to improve the interfacial adhesion of the fibers [2]. Houshyar et al. have synthesized a fiber composite using PP fibers in a Polypropylene – co - polyethylene (PPE) matrix [3]. Several methods for improving interfacial compatibility of the fiber and the matrix have been employed and evaluated by Bledzki et al. They have composited natural vegetable fibers with several polymer matrices, but faced difficulty in adhesion of the fibers and the matrix due to poor wettability and high moisture adhesion. They have circumvented this problem by using coupling agents and also used stearic acid to modify the fibers [4]. Lopez - Manchando et al. have studied the change in the mechanical and thermal properties of the composites made by adding short strands of PET and nylon 6 in isotactic PP. They have modified these fibers using p-sulphonyl-carbonyl diazide of benzoic acid as a modifying agent, which resulted in improved mechanical properties [5]. Calabia et al. have even used cotton fibers treated with VTMO to reinforce poly (butylene succinate), which is biodegradable in nature while improving the strength of the composite [6]. Wu et. al. have studied a wood plastic composite in which they developed in situ PET microfibrils with less than 500nm diameter by blending non compatible PET and HDPE phases. Further, they made a hybrid by mixing with wood flour particles resulting in a composite having much higher tensile and flexural strength [7]. Deepak et. al. have investigated the effect of reinforcing HDPE with sisal fibers. They have treated the fibers with alkali and maleic anhydride. They have also

found that adding benzoyl peroxide as an initiator helps in increasing the strength by improving grafting of maleic anhydride on HDPE [8]. Another interesting paper by Chen et. al. discusses use of hot air to partially oxidise wood fibers in conjunction with silane coupling agents to improve compatibility and thereby enhancing mechanical performance of HDPE wood fiber composite [9]. Yu et. al. have developed a composite by grafting HDPE with vinyltrimethoxysilane (VTMO). They have utilized silica as a reinforcement and used VTMO which helped in improving mechanical properties [10]. Many researchers have also tried to make composites of HDPE with PET & PP fibers and further addition of wood flour using single step injection moulding process. This aided in recycling of thermoplastic fibers [11].

In our study, PET fibers have been used to improve the mechanical properties of HDPE. It was expected that PET fibers would help in uniform distribution of stress throughout the matrix resulting in improved mechanical properties of the composite. In order to improve dispersion and adhesion between the fiber and matrix, VTMO has been used and its benefit was evaluated. Satapathy et al., 2008 have improved the mechanical performance of their composite using Maleic Anhydride grafted HDPE with PET fibers [12]. In our work, the orientation of fibers in the matrix plays an important role in distributing stress equidimensionally. The extruded composite have been injection moulded to ensure uniaxial orientation of fibers in melt resulting in improved mechanical properties. Here, the mechanical and thermal properties of the composite depend on the adhesion, dispersion and orientation of the fibers.

2. Material and Methods

2.1. Material

Material used in this work include HDPE procured from GAIL (India) Ltd., India having Melt Flow Index of 0.5g / 10 min (21.6 Kg, 190 °C), and continuous monofilament of PET fibers having diameter of 20 µm from Reliance Industries Limited. Also, coupling agent Vinyl Trimethoxy Silane (VTMO) from Evonik, India and Benzoyl peroxide initiator from SD Fine Chemical, Mumbai were obtained to initiate the coupling reaction.

2.2. Method

2.2.1 Treatment of Fibers: The PET monofilaments were hand cut into strands of 6 - 7 mm in length before treatment. The fibers were then soaked in a solution of VTMO and iso propyl alcohol (IPA), which was used as a diluent to be evaporated later. VTMO was maintained at 1 wt.% of the batch. The fibers were soaked for 24 hours, followed by drying in an air-circulating oven at 60 °C for 12 hours to remove traces of volatile IPA. Then these fibers were subjected to movement in a high speed mixer to separate the fibers from an aggregated form.

2.2.2 Preparation of Composite: The fibers were separated and tumbled with the HDPE granules and 0.1 wt.% of benzoyl peroxide initiator. The fiber loading was varied in all batches as 1%, 3%, 5%, 7%, 10%, and 15%, all on weight basis. This material was then melt blended in a twin screw co - rotating, intermeshing type APV (England) Extruder at constant screw speed of 75 rpm. The temperatures were maintained between 160 °C to 220 °C. The extruded strands were passed through a trough containing water at around 50 °C to initiate the adhesion of VTMO grafted PET fibers to HDPE. These strands were pelletized in an inline pelletizer and then subjected to drying in an air circulation oven at 70 °C. These dried pellets were injection moulded into specimens for mechanical testing in an Arburg 60 ton injection moulding machine at temperatures of 220 °C. These moulded specimens were allowed to condition at room temperature for 24 hours before carrying out the impact, tensile and flexural testing.

2.3 Characterizations

2.3.1 Mechanical Testing: The extruded pellets were injection moulded into specimens in accordance with ASTM D 638 (type I) for tensile testing, D 790 for flexural testing and D 256 for izod impact testing. For tensile testing, the load was applied at the rate of 10 mm / min, while the loading rate for flexural testing was set to 2 mm / min on a Lloyds LR 50 K Universal Testing Machine fitted with a 5 kN load cell. The izod impact testing was carried out on a Ceast Impact Tester fitted with a pendulum hammer having 2 J energy. Notch was cut on the specimen using a notch cutter in accordance to requirements of ASTM D 256. Average values of 4 tests are reported.

2.3.2 Differential Scanning Calorimetry (DSC): DSC of all sample were carried out in a TA Instruments Q 100 DSC to study the effect of addition of fibers on the crystallinity of the fiber composite. Parameters such as Melting temperature (T_m), Crystallization Temperature (T_c), Percentage of Crystallinity (X_c) were analyzed. Heating and cooling rates were maintained at 20 °C / min under an inert atmosphere of nitrogen maintained at 50 ml / min. Percentage crystallinity were calculated using the following equation [13] :

$$X_c = (\Delta H_f / \Delta H_{f0}) \times (1/W_f) \times 100$$

where, X_c is percentage of crystallinity

ΔH_f is heat of fusion

ΔH_{f0} is standard heat of fusion of 100% crystalline HDPE taken as 293 J/g

W_f is weight fraction of HDPE in composite

2.3.3 X - Ray Diffraction Spectroscopy (XRD): This testing was carried out on a Rigaku Miniflex table top XRD having Cu source with wavelength of 1.5418 Å. The specimen used was in the form of a sheet of 12.5 mm X 12.5 mm with thickness of 2 mm. The scan was performed from 5° to 80° at a rate of 3° / min. Here Scherrer's Equation was used to predict the average size of the crystal formed [14].

$$\tau = (K \lambda) / (\beta \cos \theta)$$

where, τ = mean size of crystalline domains

K = Dimensionless shape factor generally taken as 0.9

λ = X ray wavelength

β = Full width half maximum (FWHM) intensity in rads denoted as $\Delta (2\theta)$

θ = Bragg's angle

2.3.4 Dynamic Modulus: This testing was carried out on Anton Paar MCR 101 Oscillatory Rheometer at 220°C, which was the processing temperature used. Composite samples of 2 mm thickness and 25mm diameter were subjected to this test. The gap between the spindle and the base was maintained at 1 mm. From this test, the storage and loss modulus with respect to change in angular frequency were studied.

2.3.5 Scanning Electron Microscopy (SEM): The cross section of the tensile fractured specimen was visualized on a FEI Quanta 200 ESEM without the need for any sputter coating. The scanning was carried out in low vacuum resulting in high contrast images being obtained at 20 kV without charring the sample.

2.3.6 Thermogravimetric Analysis (TGA): The injection moulded samples were subjected to Thermogravimetric Analysis in a Perkin Pyris 1 instrument with heating rate at 30°/min from room temperature to 600°C under a nitrogen atmosphere.

3. Results and Discussion

3.1 Mechanical Testing: Table 1 shows the effect of addition of treated fibers on the Tensile strength, Young's modulus, strain, Flexural strength and Impact strength.

Table 1: Effect of treated PET fiber addition on mechanical properties of composite

Fiber Loading wt. %	Tensile Strength MPa	Young's Modulus MPa	% Strain at max. load	Flexural Strength MPa	Impact Strength J / m
0	26.020	202.942	10.65	32.47	350.679
1	28.329	216.240	12.48	30.02	308.539
3	29.650	221.264	12.37	31.58	267.77
5	26.743	198.513	9.67	29.88	291.048
7	24.010	117.690	9.31	30.95	240.431
10	23.240	111.739	9.95	33.37	149.056
15	23.580	122.27	8.54	32.82	112.46

Addition of treated fiber resulted in increasing of Tensile strength, Young's modulus and Flexural strength of the composite up to a loading of 3%. It is possible that as all fibers in different proportions have been treated with same amount of VTMO, the effect of VTMO to reduce the oleophobicity of the fibers has reduced leading to aggregation of fibers and subsequent loss in mechanical properties. As expected, addition of fibers results in increasing the stiffness of the composite, which led to reduction in elongation values. Decreased Izod Impact strength can be attributed to the increasing stiffness of the material, due to which the material absorbed lesser impact energy.

3.2 Differential Scanning Calorimetry:

For DSC, a carefully weighed sample of 5 - 7 mg was kept in a aluminium pan, and alongside a reference pan was kept for analysis. Heating was applied at the rate of 20 °C / min from 40 °C to 200 °C, which resulted in the melting of sample. Further, on cooling from 200 °C to 50 °C, the crystallization curve was obtained.

It can be observed from the above Table 2 that addition of treated fibers results in reduction of crystallinity of the sample. Here, the dispersed fibers adsorb themselves on the surface of the polymer molecule. This prevents the polymeric chains from coiling onto each other, thereby restricting the growth of crystallites and ultimately reducing the crystallinity of the material. This also affects the onset of melting, as can be observed from the above table. The onset of melting increases due to positive interactions of the fiber and matrix happened due to enhanced coupling by VTMO, and further reduces beyond 7% which is again due to reduced crystallinity of the material. Also, the increased loading of fibers resulted in agglomeration of fibers leading to poor heat transfer within the matrix. From the cooling cycle, it can be observed that the onset of crystallization is not much affected at the selected rate of cooling. From DSC, it can be concluded that the fibers are dispersed within the matrix and interfering in the crystallization process resulting in reduced crystallinity of the material. Figure 1. shows the DSC thermogram indicating the above trend.

Table 2: Effect of addition of fibers on crystallinity, Tm & Tc

Fiber Loading wt. %	Melting Temperature °C	Crystallization Temperature °C	Percentage Crystallinity %
0	132.90	116.23	50.40
1	131.98	114.24	47.15
3	133.37	114.16	47.53
5	133.71	114.68	48.53
7	133.37	114.25	34.52
10	130.88	115.03	37.77
15	130.83	114.24	36.26

3.3 X Ray Diffraction Spectroscopy: Using this technique, the average size of crystallite has been predicted from the Half Width Full Maximum (FWHM) values in Scherrer's equation as per the method discussed earlier. From table 3, it can be observed that the average crystal size reduces up to a fiber loading of 5%, and with more addition, the size goes on increasing. This effect can be corroborated with the FTIR result which shows good fiber and matrix interaction up to 5% loading of treated fibers, beyond which the interaction decreases.

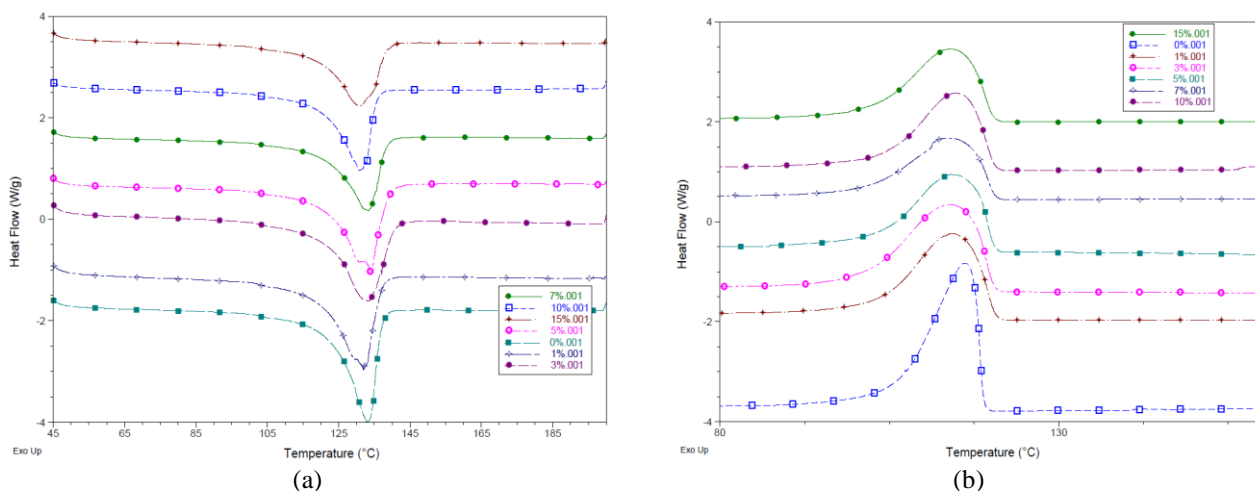


Figure 1: DSC Thermogram of composite samples (a-Melting Behavior, b-Crystallization Behavior)

This in turn has reduced the tendency of the fibers to get adsorbed on the polymer chain resulting in lesser tendency to crystallize.

3.4 Dynamic Modulus Testing:

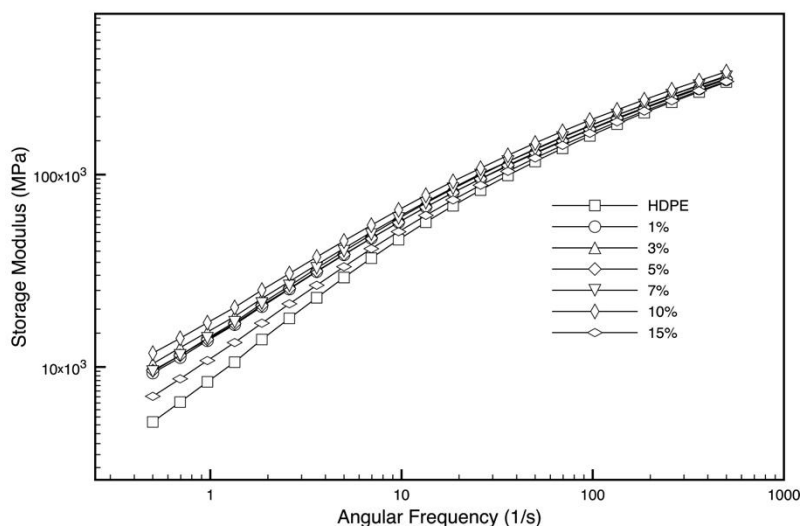
In this testing, a 2mm sheet was subjected to oscillatory movements of a parallel plate rheometer spindle within a specified frequency sweep. The data collected was plotted as Storage modulus and Loss Modulus vs. the sweep frequency.

Table 3: Effect of addition of fibers on crystal size

Fiber Loading wt. %	Bragg's Angle 2θ	FWHM $\Delta (2\theta)$	Avg. Crystallite Size (\AA)
0	22.21	0.43	377.12
1	22.23	0.50	324.33
3	21.92	0.44	369.02
5	22.25	0.51	317.79
7	21.60	0.42	385.96
10	21.95	0.42	386.19
15	22.05	0.53	306.00

This testing helps in enunciating the mechanical behavior of a composite at a molecular level. The energy stored by the molecule is called Storage Modulus (E') and energy dissipated by the molecule is called Loss Modulus (E''). Their ratio gives the $\tan \delta$ or loss factor, sometimes also called the damping coefficient.

The storage modulus gives an idea about the elastic nature of the bulk of the material, while the loss modulus gives idea about the viscous (flowable) tendency of the material. Ideally, a material demonstrates better mechanical performance when the energy storage capacity of the material increases upto a point where the resultant strain is not large. As the strain increases, the material loses energy by getting deformed and ultimately fails [15].

**Figure 2:** Storage Modulus of the composites

From Figure 2, it can be seen that addition of fibers uniformly increases the storage modulus of the material indicating a positive reinforcing tendency of the treated PET fibers. This has also resulted in increased rigidity of the material. [15].

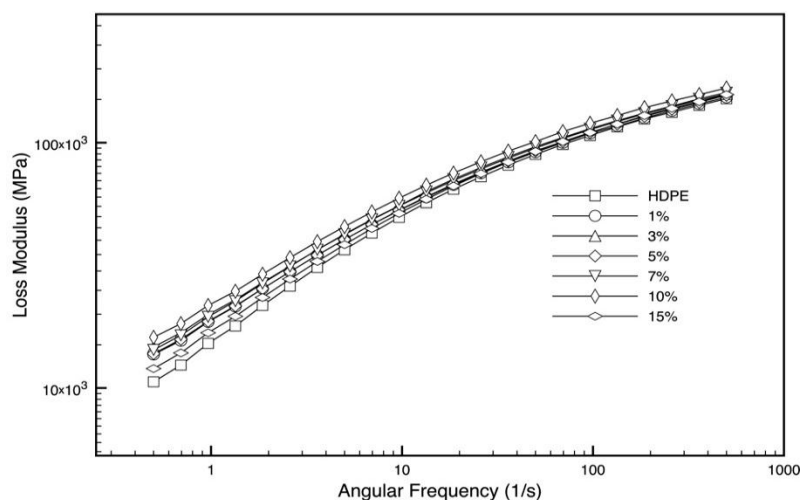
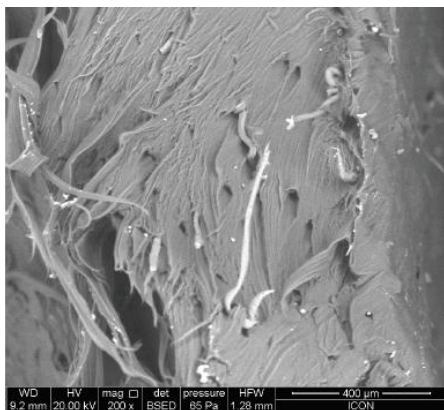
**Figure 3:** Loss Modulus of the composites

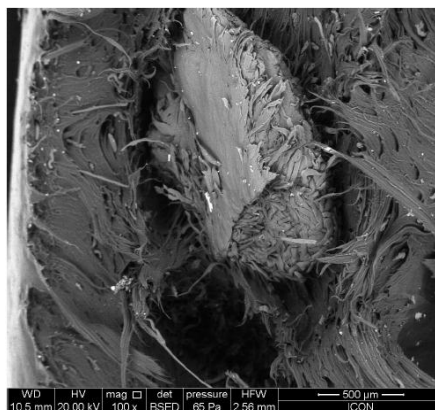
Figure 3 shows that the Loss Modulus (E'') increases with addition of fibers which establishes that the energy dissipation mechanism of the composite is not affected by addition of the fiber, and hence it can be used as reinforcement.

3.5 Scanning Electron Microscopy:

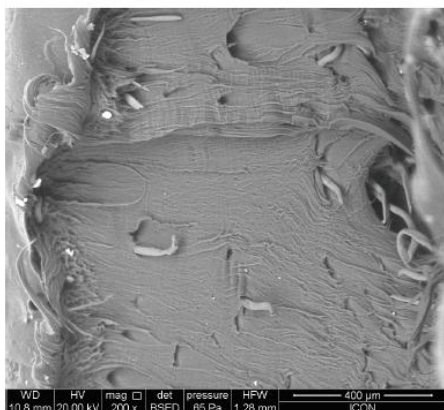
Figure 4 (a) Shows the tensile fractured surface of 3% fiber loaded composite. Under tensile loading, fibers seem to have been pulled out of the matrix leaving holes on the surface of the matrix. Figure 4 (b) Shows the fibers to be separate, and no entanglement is seen indicating good dispersion during extrusion blending. Also, the fracture surface appears clean showing increased stiffness of the composite on addition of the treated PET fibers. Pull out holes created in absence of fibers in the matrix open unidirectionally indicating good orientation of fibers during injection moulding. Figure 4 (c) shows necking of fiber indicating strain due to some degree of adhesion between treated PET fiber and matrix.



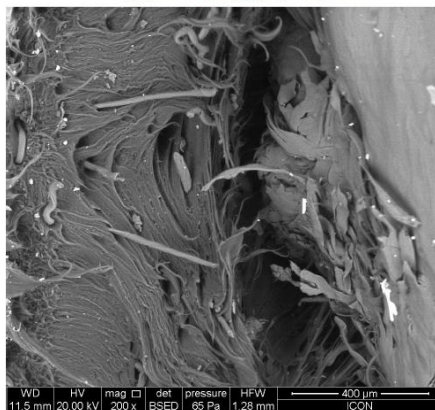
(a) Pull out hole



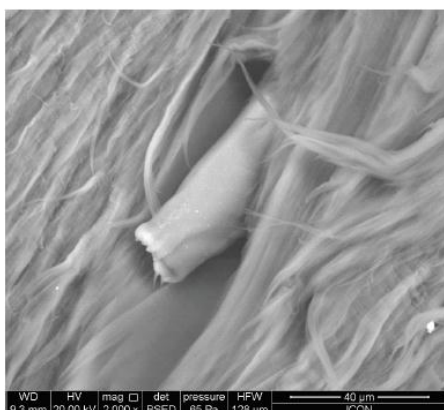
(a) Fiber agglomerates



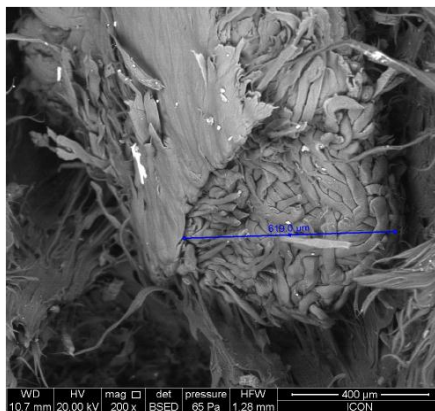
(b) Orientation of holes



(b) Void Seen



(c) Strain in fiber resulting in necking



(c) Closeup of agglomerates

Figure 4: Morphology of 3% fiber loaded composite

Figure 5: SEM morphology of 10% Composite

Figure 5 shows the fractured surface of 10% treated PET fiber loaded HDPE composite. Figure 5 (a) demonstrates presence of large agglomerates of fibers which results in points of stress concentration, thereby deteriorating the mechanical performance of the composite. Figure 5 (b) exhibits largely fractured surface with agglomerates resulting in formation of voids and Figure 5 (c) shows the closeup of the agglomerates.

3.6 Thermogravimetric Analysis:

The TGA results for 1%, 3%, 5%, 7% & 10% PET fiber filled composites have been presented in Figure 6. It has been reported in Table 5 that for 1%, 3% & 5% filled composites, the degradation onset temperature increases from 382.04 °C to 396 °C respectively.

Table 5: Thermogravimetric Analysis of Composites

Fiber Loading wt. %	Degradation Onset °C	T _{5%} °C	T _{max} °C
1	382.04	450.33	503.61
3	386.33	457.33	510.33
5	396.00	454.04	507.67
7	380.00	439.00	503.00
10	382.67	439.04	504.67

However, beyond 5% loading of PET fibers, the onset degradation temperature reduces as shown in Figure 6. This trend can be explained by corroborating the TGA results with the morphology of the composite which shows formation of agglomerates of PET fibers beyond 5% loading. The PET fibers help in improving homogeneity of the composites, thereby enabling efficient heat transfer within the matrix. However, as the fibers get entangled and subsequently agglomerated, the heat transfer within the matrix is impeded and this results in an early degradation onset of the composites.

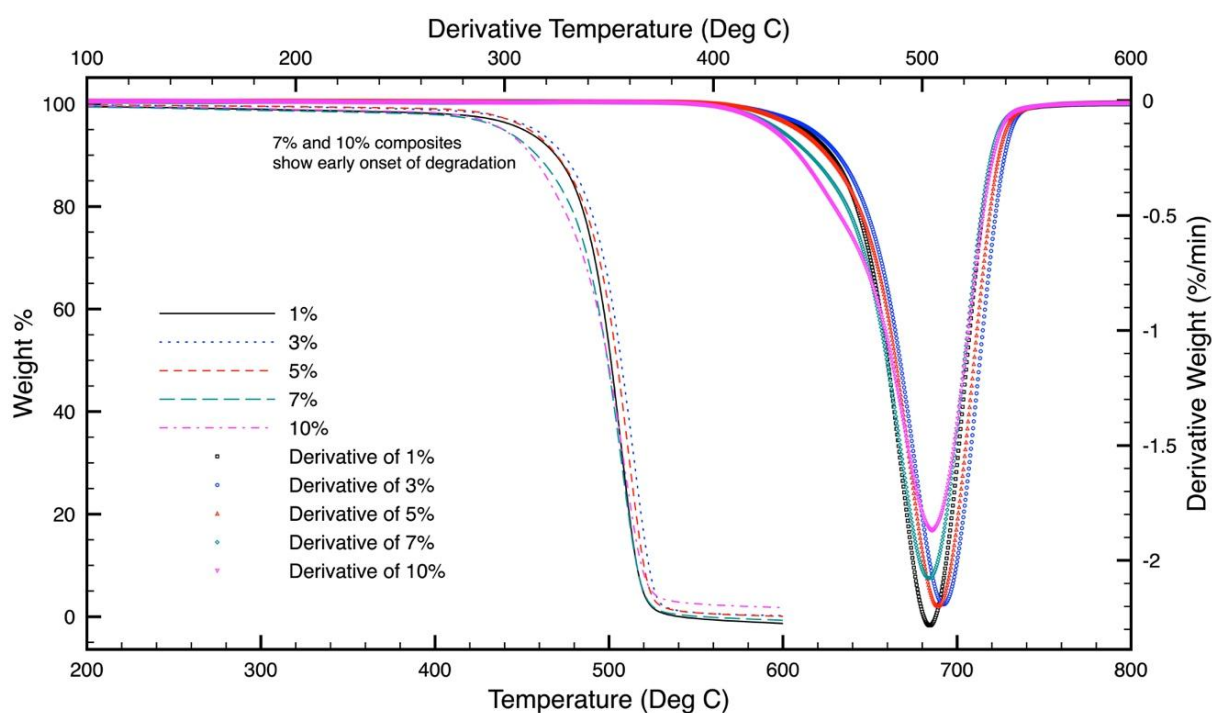


Figure 6: Thermal Gravimetry and its Derivative Curve of the Composites

Conclusion

PET microfiber based composite with HDPE has been prepared and VTMO has been evaluated as a coupling agent for this composite. Good dispersion has been obtained by the use of extrusion blending. It has been observed that VTMO treated PET microfiber helps in improving the tensile strength of the composite by 14% using 3% treated PET fiber loading, beyond which agglomeration of fibers takes place resulting in poor dispersion and deterioration of the mechanical and thermal properties. SEM has played an important role in studying the morphology of the composite and also corroborating with the mechanical and thermal properties.

References

1. M. Bengtsson, K. Oksman, The use of silane technology in crosslinking polyethylene/wood flour composites, *Composites Part A Applied Science Manufacturing*, 37 (2006), 752–65. <https://doi.org/10.1016/j.compositesa.2005.06.0144>
2. Y. Lei, Q. Wu, F. Yao, Y. Xu, Preparation and properties of recycled HDPE/natural fiber composites, *Composites Part A Applied Science Manufacturing*, 38 (2007), 1664–74. <https://doi.org/10.1016/j.compositesa.2007.02.001>
3. S. Houshyar, R. A. Shanks, A. Hodzic, The effect of fiber concentration on mechanical and thermal properties of fiber-reinforced polypropylene composites, *Journal of Applied Polymer Science*, 96 (2005), 2260–72. <https://doi.org/10.1002/app.20874>
4. A. K. Bledzki, S. Reihmane, J. Gassan, Properties and modification methods for vegetable fibers for natural fiber composites., *Journal of Applied Polymer Science*, 59 (1996), 1329–36. [https://doi.org/10.1002/\(SICI\)1097-4628\(19960222\)59:8<1329::AID-APP17>3.0.CO;2-0](https://doi.org/10.1002/(SICI)1097-4628(19960222)59:8<1329::AID-APP17>3.0.CO;2-0)
5. M. A. López-Manchado, M. Arroyo, Thermal and dynamic mechanical properties of polypropylene and short organic fiber composites. *Polymer*, 41 (2000), 7761–7. [https://doi.org/10.1016/S0032-3861\(00\)00152-X](https://doi.org/10.1016/S0032-3861(00)00152-X)
6. B. P. Calabia, F. Ninomiya, H. Yagi, A. Oishi, K. Taguchi, M. Kunioka, Biodegradable poly(butylene succinate) composites reinforced by cotton fiber with silane coupling agent, *Polymers (Basel)*, 5 (2013), 128–41. DOI: 10.3390/polym5010128
7. L. Yong, Q. Wu, High density polyethylene and poly(ethylene terephthalate) in situ sub-micro-fibril blends as a matrix for wood plastic composites, *Journal of Composites Part A*, 43 (2012), 73-78. doi:10.1016/j.compositesa.2011.09.012
8. M. Sood, D. Deepak, V. Gupta, Effect of Fiber Chemical Treatment on Mechanical Properties of Sisal Fiber/Recycled HDPE Composite, *Journal of Material Processing Proceedings*, 2 (2015), 3149-3155. doi:10.1016/j.matpr.2015.07.103
9. F. Chen, G. Han, Q. Li, X. Gao, W. Cheng, High-Temperature Hot Air/Silane Coupling Modification of Wood Fiber and Its Effect on Properties of Wood Fiber/HDPE Composites, *Journal of Materials*, 10 (2017), 286-303. doi:10.3390/ma10030286
10. W. Yu, The structure and mechanical property of silane-grafted-polyethylene/SiO₂ nanocomposite fiberrope, *Aquaculture and Fisheries* (2017), 1-5 <http://dx.doi.org/10.1016/j.aaf.2017.01.003>
11. J. Andrzejewski, M. Szostak, Preparation and Characterization of the Injection Molded Polymer Composites Based on Natural/Synthetic Fiber Reinforcement, *Advances in Manufacturing II*, 4 (2019), 473–484. https://doi.org/10.1007/978-3-030-16943-5_4
12. S. Satapathy, G. B. Nando, J. Jose, A. Nag, Mechanical Properties and Fracture Behavior of Short PET Fiber-Waste Polyethylene Composites, *Journal of Reinforced Plastic Composites*, 27 (2008), 967–84. DOI: 10.1177/0731684407086626
13. Y. Kong, J. N. Hay, The measurement of the crystallinity of polymers by DSC., *Polymer (Guildf)*, 43 (2002), 3873–8. [https://doi.org/10.1016/S0032-3861\(02\)00235-5](https://doi.org/10.1016/S0032-3861(02)00235-5)
14. L. Alexander, H. P. Klug, Determination of crystallite size with the x-ray spectrometer., *Journal of Applied Physics*, 21 (1950), 137–42. <http://dx.doi.org/10.1063/1.1699612>
15. S. Tiptipakorn, S. Rimdusit, S. Damrongsakkul, T. Kitano, Thermomechanical and rheological behaviours of waste glass fibre-filled polypropylene composites., *Engineering Journal*, 13 (2009), 45–56. DOI: 10.4186/ej.2009.13.3.45

(2019) ; <http://www.jmaterenvirosci.com>